Precision-cut tissue slices: a novel ex vivo model for fibrosis research

Pham, Bao Tung

Chapter 3

Precision-cut rat, mouse and human intestinal slices as novel models for the early-onset of intestinal fibrosis

B. T. Pham, W. T. van Haaften, D. Oosterhuis,
J. Nieken, I. A. M. de Graaf, and P. Olinga

Physiological Reports 2015, *3*(4), e12323–e12323.

ABSTRACT

Background: Intestinal fibrosis (IF) is a major complication of inflammatory bowel disease. IF research is limited by the lack of relevant *in vitro* and *in vivo* models. We evaluated precision-cut intestinal slices (PCIS) prepared from human, rat and mouse intestine as *ex vivo* models mimicking the early-onset of (human) IF.

Methods: PCIS prepared from human (h), rat (r) and mouse (m) jejunum, were incubated up to 72 h, the viability of PCIS was assessed by ATP content and morphology, and the gene expression of several fibrosis markers was determined.

Results: The viability of rPCIS decreased after 24 h of incubation, while mPCIS and hPCIS were viable up to 72 h of culturing. Furthermore, during this period, gene expression of heat shock protein 47 and plasminogen activator inhibitor 1 increased in all PCIS in addition to augmented expression of synaptophysin in hPCIS, fibronectin (*Fn2*) and *Tgfβ1* in rPCIS, *Fn2* and connective tissue growth factor (*Ctgf*) in mPCIS. Addition of TGFβ1 to rPCIS or mPCIS induced the gene expression of the fibrosis markers *Pro-collagen1a1*, *Fn2* and *Ctgf* in both species. However, none of the fibrosis markers was further elevated in hPCIS.

Conclusions: We successfully developed a novel *ex vivo* model that can mimic the early-onset of fibrosis in the intestine using human, rat and mouse PCIS. Furthermore, in rat and mouse PCIS, TGFβ1 was able to even further increase the gene expression of fibrosis markers. This indicates that PCIS can be used as a model for the early-onset of IF.

INTRODUCTION

Intestinal fibrosis (IF) is a major complication that can occur in inflammatory bowel disease (IBD), after radiation therapy or transplantation. IF is a result of chronic inflammation or injury and originates from inflammatory and immune processes acting simultaneously on many different cell types (Rieder and Fiocchi, 2009). The imbalance between inflammation/injury and tissue repair leads to excessive accumulation of collagen, fibronectin and other extracellular matrix (ECM) proteins (Rieder et al., 2007). Due to the luminal structure of the intestine, thickening of its wall by fibrosis causes stenosis, eventually requiring surgical intervention (Froehlich et al., 2005). In Crohn's Disease (CD), progressive IF leads to symptomatic bowel strictures and stenosis due to narrowing of the lumen in 30% of patients (Silverstein et al., 1999). Despite major pharmacological advances in the inflammatory component of the disease, the incidence of stricture formation in CD has not markedly changed in the past 10 years (Latella et al., 2013). CD patients that barely suffer from inflammation can still have extensive degrees of fibrosis and stenosis and vice versa (Louis et al., 2001). These findings suggest that distinct mechanisms of inflammation and restitution/fibrosis exist. Up to now, the mechanism underlying IF is still not fully understood and there is no pharmacological therapy to prevent and/or cure the fibrotic state.

Lack of knowledge about the mechanism of IF is a considerable limitation in developing antifibrotic drugs because suitable drug-targets need to be unraveled. Furthermore, the currently used (human) *in vitro* and animal *in vivo* models, mainly rodent, are not representative for the (patho)physiology of IF in human (Fiocchi and Lund, 2011). The *in vivo* animal models provoke substantial discomfort to the animals and require large numbers of animal experiments (Rieder et al., 2012). In addition, available *in vitro* and cell-culture models cannot imitate the physiologic milieu, especially not cell-cell and cell-extracellular matrix interactions between fibroblasts, stellate cells, bone marrow-derived cells, fibrocytes and pericytes (Rieder and Fiocchi, 2008). One of the most important profibrotic cytokines in IF is transforming growth factor-β1 (TGFβ1) (Lund and Rigby, 2008). Through the phosphorylation of Smad proteins, TGFβ1 can activate the downstream signaling including the expression of plasminogen activator inhibitor 1 (PAI-1) (Kutz et al., 2001). Many of its downstream effects leading to deposition of ECM, are mediated

by connective tissue growth factor (CTGF) (Dendooven et al., 2011; Latella et al., 2013). Phenotypically altered resident fibroblasts can turn into myofibroblasts that start to express alpha-smooth muscle actin (αSMA) and to produce excessive amounts of ECM. This ECM mainly consists of collagen, fibronectin (FN2) and elastin (ELA) (To and Midwood, 2011). The maturation of collagen is facilitated by heat shock protein 47 (HSP47*)* for which collagen is the only substrate (Taguchi and Razzaque, 2007). Furthermore, stellate cells which have been confirmed to play a role in liver fibrosis (Synaptophysin (SYN) is a marker), are proposed to play a role in intestinal fibrosis (Cassiman et al., 1999; Fiocchi and Lund, 2011; van de Bovenkamp et al., 2006). To be able to study the complex interplay between various intestinal cell types, an *ex vivo* (human) system which can mimic the multi-cellular process, namely precision-cut intestinal slices (PCIS), was used (de Graaf et al., 2010). PCIS have been used as a model to study drug metabolism (van de Kerkhof et al., 2008a), xenobiotic interactions and drug transport (Niu et al., 2013; Possidente et al., 2011; Vickers and Fisher, 2005). Furthermore, precision-cut tissue slices from various organs have been successfully used as a model to study fibrosis and the efficacy of antifibrotic compounds (Westra et al., 2013). In PCIS, all intestinal cell types are kept in their original tissue-matrix environment and structure. Thus, cell-cell and cell-ECM interactions are retained. Furthermore, the villus and microvillus organization is preserved, which is essential for the migration and transformation of intestinal cells (Graaf et al., 2007; Niu et al., 2013; Westra et al., 2013).

The aim of this study was to evaluate PCIS prepared from human, rat and mouse, as a novel model to mimic the early-onset of (human) IF. This model could be used to unravel the mechanism of intestinal fibrosis as well as to test the efficacy of antifibrotic compounds *ex vivo*. Firstly, the viability and morphology of PCIS were studied during culture. Secondly, the gene expressions of above mentioned fibrosis markers (*CTGF, αSMA, Pro-collagen 1a1 (COL1A1), FN2, HSP47, ELA, PAI-1, TGFβ1* and *SYN*) were determined in PCIS in the presence and absence of the fibrogenic factor TGFβ1.

MATERIAL AND METHODS

Preparation of rat and mouse intestinal cores

Adult non-fasted male Wistar rats and C57BL/6 mice were used (Harlan PBC, Zeist, The Netherlands). The rats and mice were housed on a 12 h light/dark cycle in a temperature and humidity controlled room with food (Harlan chow no 2018, Horst, The Netherlands) and water *ad libitum*. The animals were allowed to acclimatize for at least seven days before the start of the experiment. The experiments were approved by the Animal Ethical Committee of the University of Groningen.

Rats and mice were anaesthetized with isoflurane/O_2 (Nicholas Piramal, London, UK). Rat jejunum (about 25 cm distal from the stomach and 15 cm in length) and mouse jejunum (about 15 cm distal from the stomach and 10 cm in length) were excised and preserved in ice-cold Krebs-Henseleit buffer (KHB) supplemented with 25 mM D-glucose (Merck, Darmstadt, Germany), 25 mM $NaHCO_3$ (Merck), 10 mM HEPES (MP Biomedicals, Aurora, OH, USA), saturated with carbogen (95% O_2/5% CO_2) and adjusted to pH 7.4. The jejunum was cleaned by flushing KHB through the lumen and subsequently divided into 2 cm segments. These segments were filled with 3% (w/v) agarose solution in 0.9% NaCl at 37°C and embedded in an agarose core-embedding unit (de Graaf et al., 2010).

Preparation of human intestinal cores

Healthy human jejunum tissue was obtained for research from intestine that was resected from patients who underwent a pancreaticoduodenectomy. The experimental protocols were approved by the Medical Ethical Committee of the University Medical Center Groningen.

The healthy jejunum was preserved in ice-cold KHB until the embedding procedure (de Graaf et al., 2010; Roskott et al., 2010). The submucosa, muscularis and serosa were carefully removed from the mucosa within an hour after collection of the tissue. The mucosa was divided into 0.4 cm x 1 cm sheets. These sheets were embedded in 3% agarose (w/v) solution in 0.9% NaCl at 37°C and inserted in embedding unit (de Graaf et al., 2010).

Table 1: Characteristics of human PCIS from 9 Human donors

Human ID	Gender	Age	ATP (0h) pmol/µg protein
IH1	f	73	4.70
IH2	f	80	1.60
IH3	m	68	1.70
IH4	f	66	7.90
IH5	m	33	2.30
IH6	f	66	4.18
IH7	m	53	5.36
IH8	f	71	3.10
IH9	m	53	3.71

Preparation of PCIS

PCIS were prepared in ice-cold KHB by the Krumdieck tissue slicer (Alabama Research and Development, USA). The slices with a wet weight of 3-4 mg had an estimated thickness of 300-400 µm (de Graaf et al., 2010). Slices were stored in ice-cold KHB until the start of the experiments (de Graaf et al., 2010).

Incubation of intestinal slices

Slices were incubated in 12-well plates for human PCIS (hPCIS) and rat PCIS (rPCIS) or in 24-well plates for mouse PCIS (mPCIS). hPCIS and rPCIS were incubated individually in 1.3 ml and mPCIS in 0.5 ml of Williams Medium E with L-glutamine (Invitrogen, Paisley, UK) supplemented with 25 mM glucose, 50 µg/mL gentamycin (Invitrogen) and 2.5 µg/mL amphotericin-B (Invitrogen). During incubation (at 37^{o}C and 80% O_2/5% CO_2) in an incubator (MCO-18M, Sanyo), the plates were horizontally shaken at 90 rpm (amplitude 2 cm). rPCIS were incubated up to 24 h, mPCIS and hPCIS were incubated up to 72 h, with and without human TGFβ1 (Roche Diagnostics, Mannheim, Germany) in the concentration range from 1-10 ng/mL. All incubations were performed manifold (using 3-6 slices incubated individually in separate wells) and were repeated with intestine from 3 to16 different humans, rats or mice.

Viability and morphology

The viability was assessed by measuring the adenosine triphosphate (ATP) content of the PCIS, as was previously described (de Graaf et al., 2010). Briefly, after incubation, slices were transferred to 1 ml sonication solution (containing 70% ethanol and 2 mM EDTA), snap-frozen in liquid nitrogen and stored at -80ºC. To determine the viability, ATP levels were measured in the supernatant of samples sonicated for 45 seconds and centrifuged for 2 minutes at 4ºC at 16.000 x g, using the ATP bioluminescence kit (Roche Diagnostics, Mannheim, Germany). ATP values (pmol) were normalized to the total protein content (µg) of the PCIS estimated by Lowry method (BIO-rad RC DC Protein Assay, Bio Rad, Veenendaal, The Netherlands). Values displayed are relative values compared to the related controls.

To assess the morphology, incubated slices were fixed in 4% formalin and embedded in paraffin. Sections of 4 µm were cut and stained with hematoxylin and eosin (HE) (de Graaf et al., 2010). HE sections were scored according to a modified Park score, describing the sequence of development of tissue injury in the intestine after ischemia and reperfusion (Park et al., 1990; Roskott et al., 2010). The integrity of 7 segments of the PCIS were scored on a scale from 0 to 3. Viability of the epithelium, stroma, crypts and muscle layer were scored separately rating 0 if there was no necrosis, and 3 if massive necrosis was present. The other parts of the intestinal slice were rated as follows: Shape of the epithelium: 0 = cubic epithelium, 3 = more than 2/3 of the cells are flat, flattening of the villi: 0 = normal, 3 = more than 2/3 of the villi are flattened, and the amount of edema: 0 = no edema, 3 = severe edema. A maximum score of 21 indicates severe damage. In human samples, the morphological score of muscularis mucosae was determined in the 'muscle layer' section. B.T.P., W.T.v.H. and J.N. performed the blind scoring; the mean of three total scores was calculated.

Gene expression

After incubation, slices were snap-frozen in liquid nitrogen and stored at -80ºC until RNA isolation. Firstly, total RNA of three to six pooled snap-frozen slices was isolated using Qiagen RNAeasy mini kit (Qiagen, Venlo, The Netherlands). The amount of isolated RNA was measured with the BioTek Synergy HT (BioTek Instruments, Vermont, USA). Afterwards, reverse transcriptase was performed with

1 µg RNA using Reverse Transcription System (Promega, Leiden, The Netherlands). The reverse transcript polymerase chain reaction (PCR) reaction was performed in the Eppendorf mastercycler with the following gradient: 25ºC for 10 minutes, 45ºC for 60 minutes and 95ºC for 5 minutes.

The expression of the fibrosis genes, namely *COL1A1*, *αSMA*, *HSP47*, *CTGF*, *FN2, TGFβ1, PAI-1* and *SYN* were determined by either the TaqMan or SYBRgreen method. In hPCIS, ELA gene expression was also measured by SYBRgreen method. With the TaqMan method, the primers (50 µM) and probes (5 µM) listed in Table 1 were used with the qPCR mastermix plus (Eurogentec, Maastricht, The Netherlands). The real time PCR reaction was performed in a 7900HT Real Time PCR (Applied Biosystems, Bleiswijk, The Netherlands) with 40 cycles of 10 minutes at 95ºC, 15 seconds at 95ºC and 1 minute at 60ºC. With the SYBRgreen method, appropriate primers (50 µM), listed in Table 1, were used with SYBRgreen mastermix (GC Biotech, Alphen aan de Rijn, The Netherlands). The real time PCR reaction was performed with 45 cycles of 10 minutes 95ºC, 15 seconds at 95ºC and 25 seconds at 60ºC following with a dissociation stage. Ct values were corrected for the Ct values of the housekeeping gene *GAPDH* (ΔCt) and compared with the control (ΔΔCt). Results are calculated as fold induction of the gene ($2^{-\Delta\Delta Ct}$).

Statistics

A minimum of three different intestines was used for each experiment, using 3-6 slices from each intestine. The results are expressed as mean ± standard error of the mean (SEM). Differences were determined using a paired, one tailed Student's t-test and ANOVA multiple comparisons with Fisher's least significant difference test. A p-value <0.05 was considered significant. Statistical differences in ATP were determined using the values relative to the control values in the same experiment. Real-time PCR results were compared using the mean ΔΔCt values. Correlation between ATP content and mean Park score was determined using Spearman's correlation coefficient.

Table 2: Primers and probes of fibrosis markers

Primers/ Probes		Forward	Reverse	Probe
Mouse	*Gapdh*	ACAGTCCATGCCATCACTGC	GATCCACGACGGACACATTG	
	Col1a1	TGACTGGAAGAGCGGAGAGT	ATCCATCGGTCATGCTCTCT	
	αSma	ACTACTGCCGAGCGTGAGAT	CCAATGAAAGATGGCTGGAA	
	Hsp47	AGGTCACCAAGGATGTGGAG	CAGCTTCTCCTTCTCGTCGT	
	Ctgf	CAAAGCAGCTGCAAATACCA	GGCCAAATGTGTCTTCCAGT	
	Fn2	CGGAGAGAGTGCCCCTACTA	CGATATTGGTGAATCGCAGA	
	Syn	CTGTGTTTGCCTTCCTCTACTC	AGGTAGGGCTCAGACAGATAAA	
	Tgfβ1	GGTTCATGTCATGGATGGTGC	TGACGTCACTGGAGTTGTACGG	
	Pai-1	GCCAGATTTATCATCAATGACTGGG	GGAGAGGTGCACATCTTTCTCAAAG	
Rat	*Gapdh*	GAACATCATCCCTGCATCCA	CCAGTGAGCTTCCCGTTCA	CTTGCCCACAGCCTTGGCAGC
	Col1a1	CCCACCGGCCCTACTG	GACCAGCTTCACCCTTAGCA	CCTCCTGGCTTCCCTG
	αSma	AGCTCTGGTGTGTGACAATGG	GGAGCATCATCACCAGCAAAG	CCGCCTTACAGAGCC
	Hsp47	AGACGAGTTGTAGAGTCCAAGAGT	ACCCATGTGTCTCAGGAACCT	CTTCCCGCCATGCCAC
	Ctgf	ACACAAGGGTCTTCTGCGA	TTGCAACTGCTTTGGAAGGAC	
	Fn2	TCTTCTGATGTCACCGCCAACTCA	TGATAGAATTCCTTGAGGGCGGCA	
	Syn	CTTTGCCATCTTCGCCTTTG	GCCCGTAATCGGGTTGATAA	
	Tgfβ1	CCTGGAAAGGGCTCAACAC	CAGTTCTTCTCTGTGGAGCTGA	
	Pai-1	AACCCAGGCCGACTTCA	CATGCGGGCTGAGACTAGAAT	
Human	*GAPDH*	ACCAGGGCTGCTTTTAACTCT	GGTGCCATGGAATTTGCC	TGCCATCAATGACCCCTTCA
	COL1A1	CAATCACCTGCGTACAGAACGCC	CGGCAGGGCTCGGGTTTC	CAGGTACCATGACCGAGACGTG
	αSMA	AGGGGGTGATGGTGGGAA	ATGATGCCATGTTCTATCGG	GGGTGACGAAGCACAGAGCA
	HSP47	GCCCACCGTGGTGCCGCA	GCCAGGGCCGCCTCCAGGAG	CTCCCTCCTGCTTCTCAGCG
	FN2	AGGCTTGAACCAACCTACGGATGA	GCCTAAGCACTGGCACAACAGTTT	
	CTGF	ACGGCGAGGTCATGAAGAAGAACA	ACTCTCTGGCTTCATGCCATGTCT	
	SYN	CTGCACCAAGTGTACTTTGAT	GCTGACGAGGAGTAGTCCC	GGGCACCACCAAGGTC
	TGFβ1	TGGCGATACCTCAGCAACC	CTCGTGGATCCACTTCCAG	
	PAI-1	CACGAGTCTTTCAGACCAAG	AGGCAAATGTCTTCTCTTCC	
	ELA	GGCCATTCCTGGTGGAGTTCC	AACTGGCTTAAGAGGTTTGCCTCCA	

RESULTS

Viability of PCIS

The ATP content and the morphology of PCIS were used to evaluate the viability of the slices during culturing. Directly after slicing, the ATP content of the PCIS from human (h), rat (r) and mouse (m) was 3.49 ± 1.56, 4.34 ± 1.69, 3.82 ± 1.95 pmol/μg protein, respectively. No significant difference in the ATP content of PCIS from different species was found. When compared to directly after slicing, the ATP content of hPCIS decreased about 30% and 50%, after 48 and 72 h of incubation respectively (Figure 1A). However, in rPCIS, already after 4 h of incubation the ATP content significantly decreased and after 24 h the ATP content was reduced by 75% compared to freshly prepared PCIS (Figure 1B). In mPCIS, the ATP content was not significantly different after 48 h of incubation, yet, after 72 h of culturing, ATP levels were significantly decreased to 36% as compared to freshly prepared PCIS (Figure 1C).

To evaluate the morphological integrity of PCIS after incubation, the modified Park score was used. An increased Park score indicated a decrease in viability. Mean Park scores of hPCIS increased significantly during 48 h of culture when compared to hPCIS directly after slicing (Figure 2A). Furthermore, the mean Park score of rPCIS and mPCIS also increased significantly during incubation (Figure 2B, 2C). Very low Park score of non-incubated slices showed that PCIS were not damaged by handling and slicing (Figure 2). A significant correlation between ATP content and mean Park scores was found in hPCIS (Spearman $r = -0.76$, $p < 0.0001$), rPCIS (Spearman $r = -0.73$, $p =< 0.0002$) and mPCIS (Spearman $r = -0.82$, $p = 0.0033$) (Figure 2D-F)

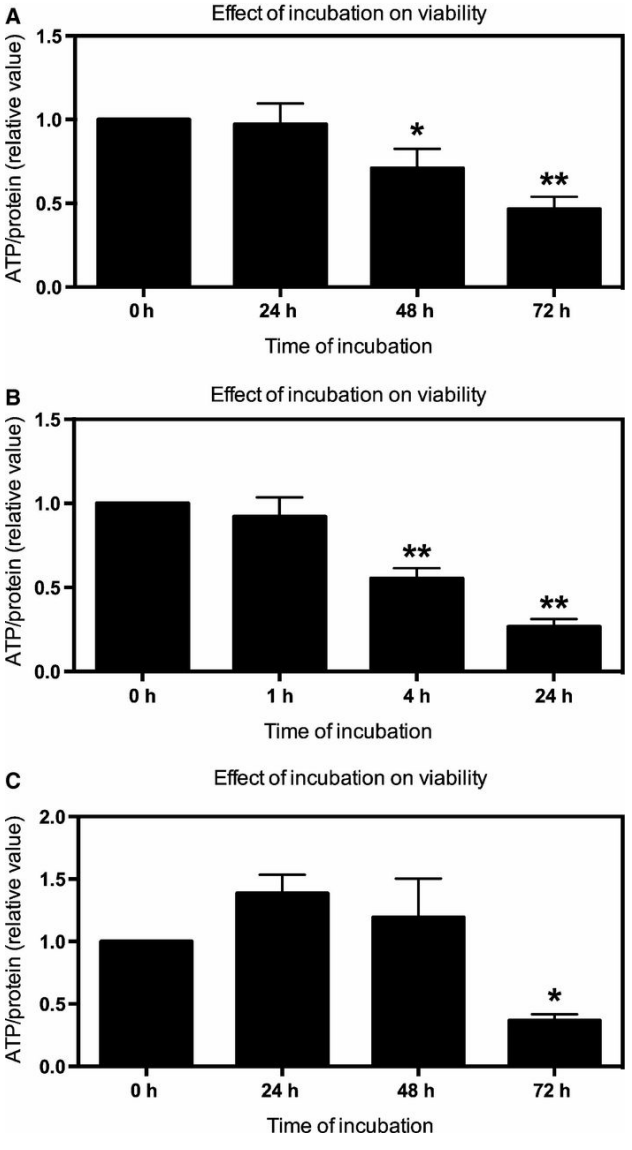

Figure 1. Long-term incubation of hPCIS, rPCIS and mPCIS. The viability of PCIS as measured by ATP content (relative value compare to 0h) after incubation of (A) hPCIS up to 72 h, (B) rPCIS up to 24 h and (C) mPCIS up to 72 h. (*$p < 0.05$, **$p < 0.01$ vs. 0 h. n = 9-15, data are expressed as mean +/- SEM).

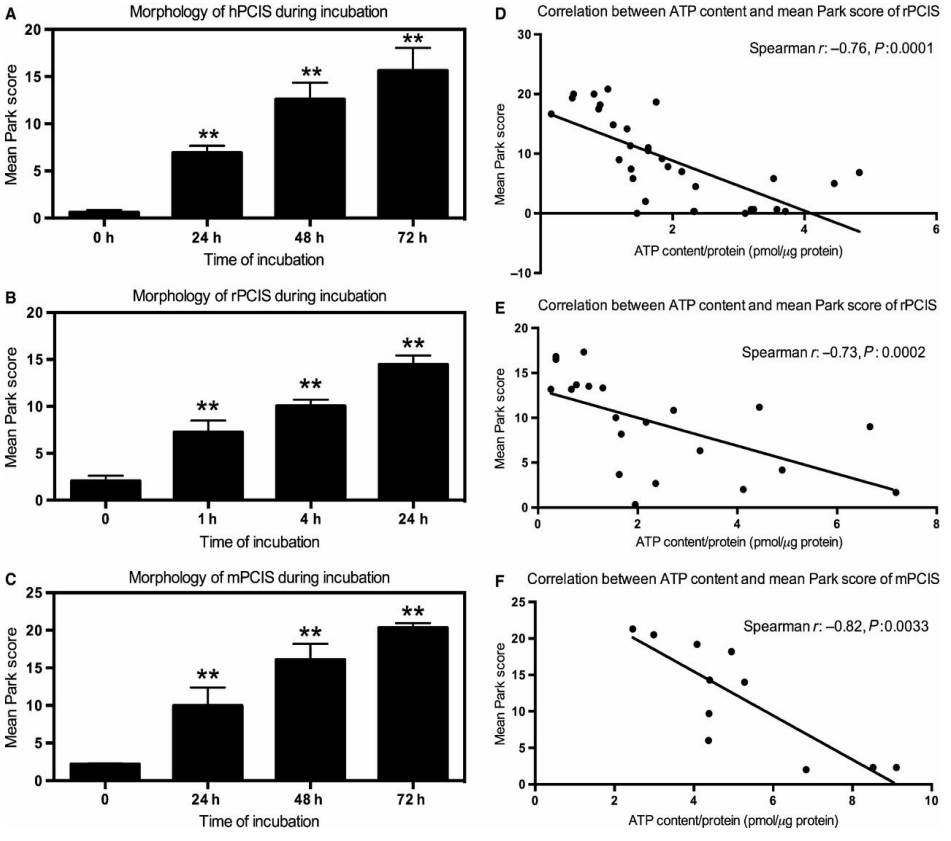

Figure 2. Park score of hPCIS, rPCIS and mPCIS after long-term incubation. Mean Park scores of (A) hPCIS, (B) rPCIS and (C) mPCIS after different incubation intervals. (by BTP, JN and WTvH, *p < 0.05, n = 5-8, data are expressed as mean +/- SEM). (D) Spearman correlation between ATP content and mean. Park score in hPCIS (r = -0.76, p < 0.0001), (E) rPCIS (r = -0.73, p =< 0.0001) and (F) mPCIS (r = -0.81, p = 0.0015).

During culturing of human, rat and mouse intestinal slices the same sequence of morphological changes and damage was found (Figure 3). Firstly, epithelial and stromal cells were damaged, with clear signs of necrosis in these cells. In association, flattening of the villi and of epithelial cells (i.e. losing their cubic shape), and development of edema was found (Figure 3B). Subsequently, necrosis was evident in cells of the crypts and the muscle layer. By incubating hPCIS up to 72 h, massive necrosis was apparent in both epithelial and stromal cells (Figure 3C). In association with necrosis, destruction of the normal tissue architecture was found as shown in Figure 3C.

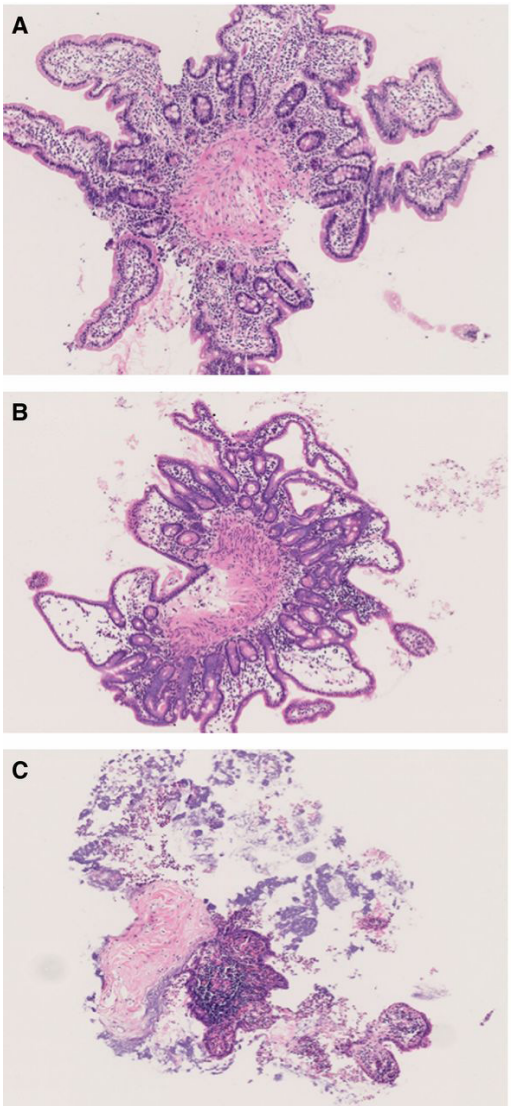

Figure 3. Morphological integrity of hPCIS after long-term incubation. HE staining of representative healthy hPCIS after (A) 0 h, (B) 48 h and (C) 72 h incubation (magnification: 4x).

PCIS of all species were incubated with TGFβ1, to confirm that PCIS can be used to study the TGFβ1 signaling pathway. hPCIS viability decreased slightly, but not significantly, after 24 h of incubation with 10 ng/mL TGFβ1. Meanwhile, when hPCIS were incubated for 48 h, TGFβ1 did not affect the hPCIS ATP content (Figure 4A). Moreover, ATP content of rPCIS did not decreased after 24 h of incubation in

the presence of up to 5 ng/ml TGFβ1 (Figure 4B). In contrast, 10 ng/ml of TGFβ1 decreased the viability of rPCIS considerably (data not shown). Meanwhile, in mPCIS, up to 48 h in culture, no effect on the viability due to TGFβ1 was observed (Figure 4C).

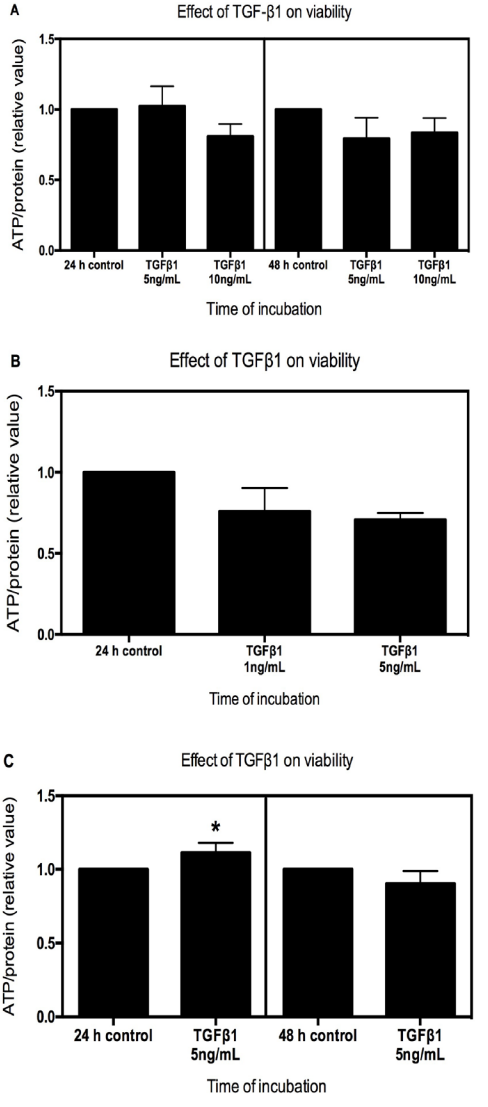

Figure 4. Long-term incubation of hPCIS, rPCIS and mPCIS with TGFβ1. The viability of PCIS as measured by ATP content (relative value compare to control) after incubation of: (A) hPCIS up to 48 h with 5 ng/mL and 10 ng/mL TGFβ1, (B) rPCIS up to 24 h with 1 ng/mL and 5 ng/mL TGFβ1 and (C) mPCIS up to 48 h with 5 ng/mL TGFβ1. (*$p < 0.05$, **$p < 0.01$ vs. control n = 3-6, data are expressed as mean +/- SEM).

Gene expression of fibrosis markers

To determine if the early-onset of fibrosis is induced in PCIS, gene expression of various fibrosis markers was investigated. After 24 h of incubation, the gene expression of an early marker of fibrosis, *HSP47,* was elevated in hPCIS when compared to hPCIS directly after slicing. *HSP47* steadily increased up to 72 h. Furthermore, when compared to hPCIS after preparation, *SYN* gene expression significantly increased in hPCIS after 48 h and was even higher after 72 h of incubation. Conversely, *ELA* expression was decreased after 48 h incubation (Figure 7E) and *αSMA* expression was down-regulated after incubation up to 72 h compared to freshly prepared PCIS (Figure 5A). Furthermore, *COL1A1, CTGF* and *FN2* expression was not affected during incubation of hPCIS (Figure 5A).

After 24 h of incubation of rPCIS, the gene expression of *Hsp47* and *Fn2* was significantly increased compared to PCIS directly after slicing. Similar to hPCIS, *αSma* was down-regulated, whereas *Col1a1*, *Ctgf* and *Syn* expression was unaffected after 24 h of culture (Figure 5B).

As was found in rPCIS the gene expression of *Hsp47* and *Fn2* was significantly increased in mPCIS after 24 h, which increased even further up to 48 and 72 h of incubation. *Ctgf* expression was only increased after 72 h of incubation in mPCIS. In contrast to the gene expression of *αSma* and *Col1a1,* which was significantly down-regulated up to 72 h in mPCIS (Figure 5C). *Syn* expression remained unchanged during incubation in both rPCIS and mPCIS.

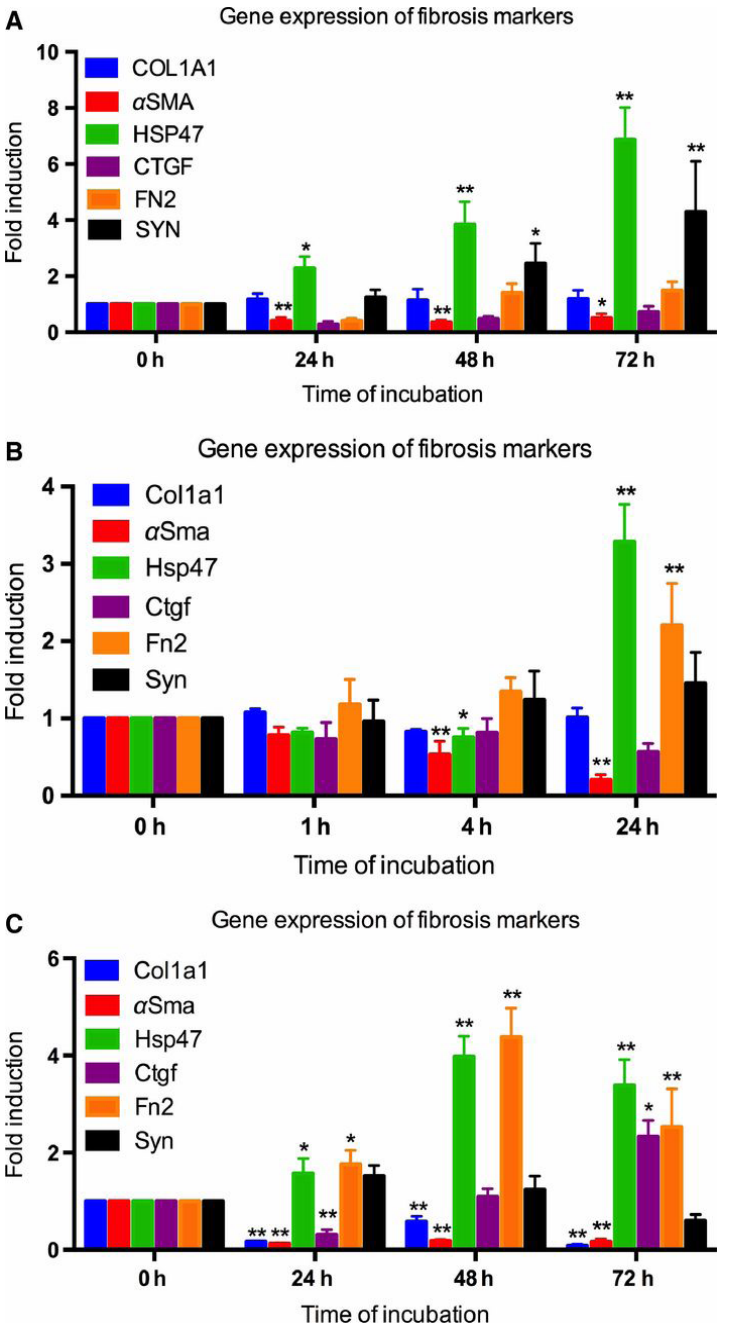

Figure 5. Gene expression of fibrosis markers in hPCIS, rPCIS, and mPCIS after long-term incubation. The gene expression of fibrosis markers *COL1A1*, *HSP47*, *αSMA*, *CTGF*, *FN2* and *SYN* after incubation of (A) hPCIS for 72 h, (B) rPCIS for 24 h, and (C) mPCIS for 48 h. (*$p < 0.05$, **$p < 0.01$ vs. 0 h. n = 3-6, data are expressed as mean +/- SEM).

Addition of TGFβ1

To study if the main fibrogenic factor TGFβ1 was able to induce fibrogenesis in these models, PCIS were incubated with TGFβ1. The gene expression of none of the investigated fibrosis markers was affected in hPCIS when incubated for 48 h with up to 10 ng/ml TGFβ1 (Figure 6A and Figure 7E). However, in rPCIS, when incubated for 24 h with 1 ng/mL TGFβ1, *Ctgf* and *Fn2* were significantly up-regulated compared to control and remain elevated in the presence of 5ng/mL TGFβ1. Meanwhile, *αSma and Col1a1* expressions were significantly increased compared to the 24 h control only, when incubated with 5 ng/mL TGFβ1. Interestingly, *Hsp47* expression in rPCIS tended to decrease with 1 ng/mL TGFβ1 and was significantly down-regulated when adding 5 ng/mL TGFβ1 during culture (Figure 6B). In mPCIS after 48 h of incubation in the presence of 5 ng/mL TGFβ1 the gene expression of *Col1a1*, *Fn2, Hsp47* and *Ctgf* was significantly up-regulated compared to the 48 h control (Figure 6C). However, *Syn* expression was not affected in both rPCIS and mPCIS in the presence of TGFβ1.

Both *TGFβ1* and *PAI-1*, the specific downstream marker of TGFβ1 signaling (22), gene expression was investigated. Only in rPCIS the *Tgfβ1* was significantly increased (Figure 7B). However, the gene expression of *PAI-1* was increased dramatically in all species suggesting activation of the TGFβ1 pathway (Figure 7A, 7B and 7C). When slices were incubated in the presence of TGFβ1, the gene expression *PAI-1* was not further increased, except for rPCIS (Figure 7D).

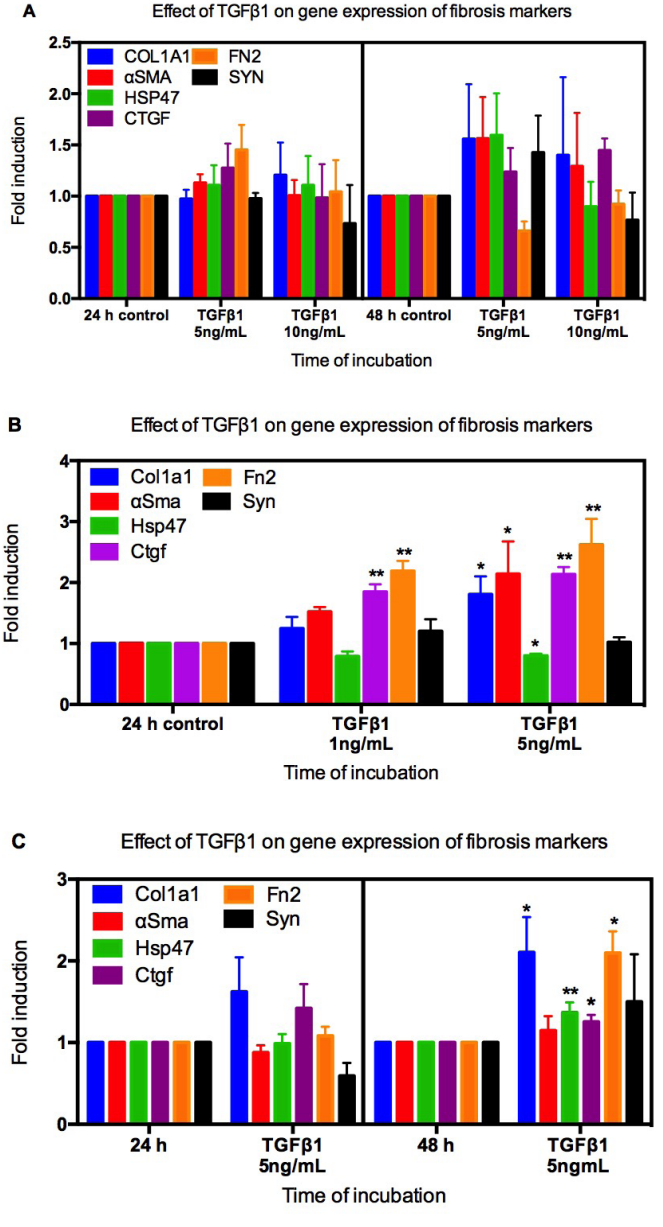

Figure 6. Gene expression of fibrosis markers in hPCIS, rPCIS, and mPCIS after long-term incubation with TGFβ1. The gene expression of fibrosis markers *COL1A1*, *HSP47*, *αSMA*, *CTGF*, *FN2* and *SYN* after incubation of (A) hPCIS for 48 h with 5 ng/mL and 10 ng/mL TGFβ1, (B) rPCIS for 24 h with 1 ng/mL and 5 ng/mL TGFβ1, and (C) mPCIS for 48 h with 5 ng/mL TGFβ1. (*$p < 0.05$, **$p < 0.01$ vs. control. n = 3-5, data are expressed as mean +/- SEM).

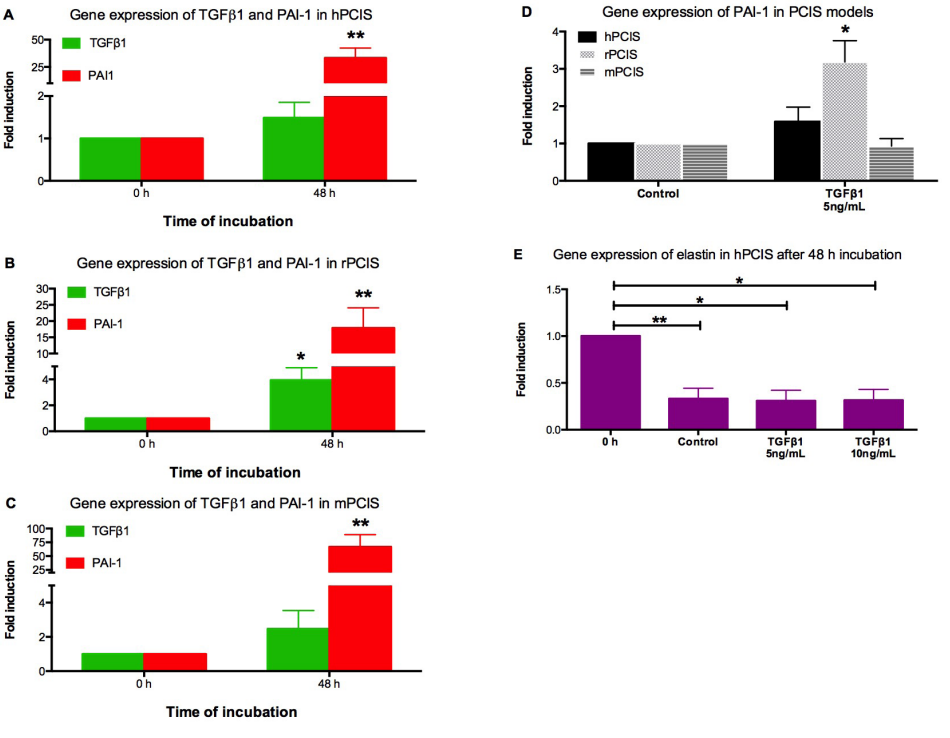

Figure 7. Gene expression of *TGFβ1* and *PAI-1* in hPCIS, rPCIS and mPCIS after long-term incubation with TGFβ1. The gene expression of fibrosis markers *TGFβ1* and *PAI-1* after incubation of (A) hPCIS for 48 h, (B) rPCIS for 24 h, and (C) mPCIS for 48 h. (D) The gene expression of *PAI-1* in PCIS models after incubation (48h with hPCIS and mPCIS, 24 h with rPCIS) with 5 ng/mL TGFβ1. (E) The gene expression of *ELA* in hPCIS model after incubation for 48 h with and without 5 ng/mL and 10 ng/mL TGFβ1 (*p < 0.05, **p < 0.01 vs. 0 h or control. n = 3-5, data are expressed as mean +/- SEM.

DISCUSSION

Intestinal fibrosis is a complicated condition, caused by extensive chronic inflammation or injury of the bowel. Although there are some animal models for IF, most of them are limited in their relevance to human disease and have some definite disadvantages, such as animal discomfort and long time needed to establish the fibrosis state (Rieder et al., 2012). Until now, there are no antifibrotic drugs available and relevant models are needed. As reviewed before, precision-cut tissue slices can provide a good model to study the early-onset of organ fibrosis (Westra et al., 2013), and can also considerably reduce the number of animals used in intestinal fibrosis research. The aim of this study was to develop a method for studying the early-onset of IF by using PCIS from various species, namely human, rat and mouse.

Viability by ATP content of PCIS

Precision-cut intestinal slices have been used previously to study drug metabolism and toxicity in the intestinal tract. In these studies, hPCIS were used to investigate the regulation, expression and capacity of metabolic enzymes, transporters and receptors indicating that PCIS can mimic the intestine *in vivo* (Khan et al., 2009; Khan et al., 2010; van de Kerkhof et al., 2006; van de Kerkhof et al., 2008b). Previously, hPCIS were incubated for a relatively short period of time (up to 24 h). To study the onset of fibrosis, we incubated PCIS for a longer period (rPCIS up to 24 h, mPCIS and hPCIS up to 72 h). ATP is used in precision-cut tissue slices from different organs as general marker of viability. To establish this in PCIS the morphology during incubation was compared to the ATP content in the slices. Morphological scoring (according to the modified Park score (Park et al., 1990; Roskott et al., 2010)) of mPCIS, rPCIS and hPCIS showed that the ATP is related to the morphological integrity of the tissue. Therefore, ATP levels in PCIS are used as a general marker for morphological integrity in different species in the current study. In addition, the sequence of losing cell integrity in PCIS from different species is similar, indicating that the same processes take place in the PCIS from all studied species. Epithelial and stromal cell damage was observed first, indicating that these cells are the most vulnerable to ischemia. This is also shown in the original article describing the Park score (Park et al., 1990). However, more specific markers for the different cell types in the PCIS are necessary to obtain information on the viability

of these cells in PCIS during culture.

The decline of ATP content found in our study was also observed in other studies with rPCIS (van de Kerkhof et al., 2007) and hPCIS (de Graaf et al., 2010). Moreover, PCIS from the different species behave differently during culture. The ATP content in PCIS directly after slicing was comparable in all species. Striking is however the species difference of the maximal incubation period of the PCIS. In rPCIS after 24 h incubation ATP content was less than 50% compared to directly after slicing, in contrast to mPCIS and hPCIS, where this value was reached only after 72 h. One of the factors may be the production of reactive oxygen species (ROS). During slicing and storage before the start of the incubation, the PCIS are subjected to ischemia. Upon culturing, the PCIS are re-oxygenated. It is known from studies in biopsies that in the rat intestine xanthine oxidase (XO) steeply increases during ischemia, which is in contrast to the human intestine (Bianciardi et al., 2004). Upon re-oxygenation, XO will lead to ROS and subsequently to cell and tissue damage (Bianciardi et al., 2004). Furthermore, *Tgfβ1* gene expression was also increase in rPCIS, possibly subsequently also TGFβ1 protein and this could lead to the production of ROS (Rhyu et al., 2005; Yan et al., 2014). This might explain why rPCIS deteriorate faster in culture than mPCIS and hPCIS. Future studies will be performed to determine ROS production in PCIS of different species.

Gene expression of fibrosis markers

The aim of our study was to induce the early-onset of fibrogenesis, which could be triggered by the loss of cell integrity over time. Therefore, we studied the gene expression of different fibrosis markers, often linked to the protein expression (Westra et al., 2014a; Westra et al., 2014b). In addition, TGFβ1 was added to the PCIS to establish if one of the main inducers of fibrogenesis is also effective in PCIS.

In hPCIS cultured up to 72 h, *HSP47* gene expression was elevated. Other studies have identified *HSP47* as a potential early marker of IF (Honzawa et al., 2010; Taguchi and Razzaque, 2007). It has been demonstrated that the serum level of *HSP47* is higher in CD patients, who are prone for IF, compared to those with ulcerative colitis, an intestinal disease that rarely leads to IF, and to control patients (Taguchi et al., 2011). Moreover, Honzawa et al. showed that *HSP47* expression contributes to IF in CD (Honzawa et al., 2014) and in the IL-10-/- mouse model

of IF, HSP47 plays an essential role (Kitamura et al., 2011; Rieder et al., 2012). Therefore, *HSP47* is a biomarker for IF and furthermore used *ex vivo* in hPCIS to study the efficacy of antifibrotic drugs (Taguchi et al., 2011).

SYN, a marker of stellate cells (Cassiman et al., 1999), was also up-regulated in hPCIS. As was reported before by Rieder et al. (Rieder and Fiocchi, 2008) stellate cells are present in the intestine and may contribute to the fibrotic process. As was shown before with hepatic stellate cells (HSCs), if the liver is injured, HSCs change their phenotype to an activated state, start to express among others *αSMA*, and to synthesize pro-inflammatory cytokines and ECM proteins (Li and Friedman, 1999). Intestinal stellate cells seem to display the same basic morphological, phenotypic, and functional characteristics as the hepatic stellate cell and recently have been isolated and cultured from mesenteric fibrotic tissue from a patient with a fibrotic carcinoid tumor (Fiocchi and Lund, 2011; Kidd et al., 2007). Therefore, the increase of stellate cell number and *HSP47* induction up to 72 h in hPCIS during culturing indicates that slices can be used as a tool to study the early stage of fibrosis.

The decrease in *αSMA* expression up to 72 h in hPCIS might be explained by a loss of fibroblasts, which was also found in other organ slices (Westra et al., 2013). In hPCIS, none of the other fibrosis markers (*COL1A1, FN2 and ELA*) were increased during culturing, even with the addition of increasing concentrations of TGFβ1. This may indicate that the TGFβ pathway cannot be induced, or is already activated due to the operation and procurement of the tissue. Moreover, it should be noted that in the intestine, the resident macrophages are mainly in the muscularis (Smith et al., 2011), which was removed from the human intestinal tissue before hPCIS were prepared. Although the mechanism of IF in human is still unknown, the spontaneous early fibrosis may require macrophages to develop. Future studies with specific inhibitors of the TGFβ pathway will elucidate if the pathway is already activated. Furthermore, maybe an additional trigger such as PDGF or the presence of the inflammatory cytokine TNF alpha is necessary to induce fibrosis in hPCIS, which has been reported in liver fibrosis and idiopathic pulmonary fibrosis (Basaranoglu et al., 2013; Kropski et al., 2012). In future experiments with PCIS it will be elucidate if a second hit is necessary. In human liver slices, not only TGFβ1 but both potent fibrogenic factors PDGF and TGFβ1 are necessary to induce gene expression of fibrosis markers (Westra et al., 2011). Research is currently ongoing to further induce the gene expression of fibrosis markers in hPCIS.

We have investigated the gene expression of *ELA* in the hPCIS. Although it has been reported that *ELA* was activated by TGFβ1 in lung fibroblasts (Kuang et al., 2007), there is no report of the involvement of elastin in fibrosis in other organs. In hPCIS, *ELA* was not induced during incubation with or without TGFβ1. This may indicate that the activation of elastin is lung specific.

In rPCIS, both *Hsp47* and *Fn2* were increased after 24 h of culture. These results imply that the early-onset of fibrogenesis is indeed induced in rPCIS during culture up to 24 h. Addition of TGFβ1 further increased *Fn2* expression, but not *Hsp47* that was down-regulated by TGFβ1. This may be explained by the fact that for the early fibrosis marker *Hsp47*, the maximum gene expression was reached earlier by adding TGFβ1 during rPCIS incubation than in the control incubation of rPCIS. This is in accordance with the results of *Col1a1*, the marker of fibrosis, that was only elevated in rPCIS by TGFβ1, as was also seen in other organ slices (Westra et al., 2011). Similarly, *Ctgf* expression was only elevated in rPCIS after the addition of TGFβ1, this is in line with the function of Ctgf in the TGF-β pathway (Brigstock, 2010). As was assessed in hPCIS, *αSma* expression was also decreased in rPCIS, indicating again that fibroblasts may be lost during culture. However, *αSma* expression was increased in rPCIS by TGFβ1. This may suggest that (myo) fibroblasts are activated by TGFβ1 in rPCIS.

In accordance with the results in rPCIS, prolonged culture of mPCIS induced *Hsp47* and *Fn2* expression, but *αSma* was decreased during culture up to 72 h. However unlike rPCIS and hPCIS, where *Col1a1* was unchanged during culture, in mPCIS the gene expression of *Col1a1* was significantly decreased. In an *ex vivo* model of liver fibrosis (Westra et al., 2014a), *Col1a1* was also down-regulated after 24 h incubation, but increased after 48 h incubation due to activation of the wound repair system (Vickers and Fisher, 2005). In mPCIS, probably longer incubation in the presence of pro-fibrotic cytokines is needed to initiate the wound healing process and fibrosis. Interestingly, only in mPCIS, *Ctgf* gene expression was up-regulated after 72 h incubation, this is an indication that the TGFβ pathway was activated after long-term incubation. Furthermore, addition of TGFβ1 to mPCIS induced gene expression of *Col1a1*, *Fn2*, *Ctgf* and even *Hsp47* that was down-regulated in rPCIS. *αSma* expression was not affected by TGFβ1 in mPCIS. In contrast to hPCIS, *Syn* was not induced in rPCIS and mPCIS, not even in the presence of TGFβ1. This suggests differences between species in the proliferation of intestinal stellate cells.

All these results imply that in rPCIS and mPCIS there was a spontaneous induction of early fibrogenesis, which can be measured by gene expression of *Hsp47* and *Fn2*. Our result of the early onset of fibrosis in PCIS are in line with the results in a liver fibrosis model using precision-cut liver slices, which we already successfully used in studying antifibrotic compounds (Westra et al., 2014a). Future studies with specific signaling pathway inhibitors will be performed to elucidate why during culturing of PCIS spontaneous induction of these markers occurs. TGFβ1 was able to even further stimulate the onset of fibrosis in rat and mouse, indicating the importance of TGFβ1 as profibrotic stimulus in rodents. Upcoming experiments have to clarify if the TGFβ1 pathway is involved in the spontaneous activation of early fibrogenesis in PCIS. Moreover, we found clear species differences in the early-onset of fibrosis, therefore, we are currently performing studies, among others by staining different intestinal cell types, to elucidate these difference.

CONCLUSION

We successfully developed a relevant *ex vivo* intestinal model in both rodent and man to study the early-onset of intestinal fibrosis. In rat and mouse PCIS, TGFβ1 was able to even further increase the gene expression of fibrosis markers. The gene expression of *HSP47* in human and rodent PCIS, and in rodent PCIS also *Fn2*, can be used as early markers of fibrosis. These results open the opportunity to test the efficacy of antifibrotic drugs in both human and rodents in an *ex vivo* physiological model. The model also provides the opportunity to study the fibrogenesis in different regions of the intestine. Furthermore, the mechanism of fibrosis in an *ex vivo* model of early fibrogenesis in different species can be determined. The research is currently expanding to the diseased human (fibrotic) intestine.

REFERENCES

1. **Basaranoglu, M., Basaranoglu, G. and Sentürk, H.** (2013). From fatty liver to fibrosis: A tale of "second hit." *World J. Gastroenterol.* **19**, 1158–1165.
2. **Bianciardi, P., Scorza, R., Ghilardi, G. and Samaja, M.** (2004). Xanthine oxido-reductase activity in ischemic human and rat intestine. *Free Radic. Res.* **38**, 919–25.
3. **Brigstock, D. R.** (2010). Connective tissue growth factor (CCN2, CTGF) and organ fibrosis: lessons from transgenic animals. *J. Cell Commun. Signal.* **4**, 1–4.
4. **Cassiman, D., van Pelt, J., De Vos, R., Van Lommel, F., Desmet, V., Yap, S. H. and Roskams, T.** (1999). Synaptophysin: A novel marker for human and rat hepatic stellate cells. *Am. J. Pathol.* **155**, 1831–9.
5. **de Graaf, I. a M., Olinga, P., de Jager, M. H., Merema, M. T., de Kanter, R., van de Kerkhof, E. G. and Groothuis, G. M. M.** (2010). Preparation and incubation of precision-cut liver and intestinal slices for application in drug metabolism and toxicity studies. *Nat. Protoc.* **5**, 1540–51.
6. **Dendooven, A., Gerritsen, K. G., Nguyen, T. Q., Kok, R. J. and Goldschmeding, R.** (2011). Connective tissue growth factor (CTGF/CCN2) ELISA: a novel tool for monitoring fibrosis. *Biomarkers* **16**, 289–301.
7. **Fiocchi, C. and Lund, P. K.** (2011). Themes in fibrosis and gastrointestinal inflammation. *Am. J. Physiol. Gastrointest. Liver Physiol.* **300**, G677–83.
8. **Froehlich, F., Juillerat, P., Mottet, C., Felley, C., Vader, J.-P., Burnand, B., Gonvers, J.-J. and Michetti, P.** (2005). Obstructive fibrostenotic Crohn's disease. *Digestion* **71**, 29–30.
9. **Graaf, I. A. de, Groothuis, G. M. and Olinga, P.** (2007). Precision-cut tissue slices as a tool to predict metabolism of novel drugs. *Expert Opin. Drug Metab. Toxicol.* **3**, 879–98.
10. **Honzawa, Y., Nakase, H., Takeda, Y., Nagata, K. and Chiba, T.** (2010). Heat shock protein 47 can be a new target molecule for intestinal fibrosis related to inflammatory bowel disease. *Inflamm. Bowel Dis.* **16**, 2004–6.
11. **Honzawa, Y., Nakase, H., Shiokawa, M., Yoshino, T., Imaeda, H., Matsuura, M., Kodama, Y., Ikeuchi, H., Andoh, A., Sakai, Y., et al.** (2014). Involvement of interleukin-17A-induced expression of heat shock protein 47 in intestinal fibrosis in Crohn's disease. *Gut* **63**, 1902–1912.
12. **Khan, A. a., Chow, E. C. Y., van Loenen-Weemaes, A. M. M. a, Porte, R. J., Pang, K. S. and Groothuis, G. M. M.** (2009). Comparison of effects of VDR versus PXR, FXR and GR ligands on the regulation of CYP3A isozymes in rat and human intestine and liver. *Eur. J. Pharm. Sci.* **37**, 115–125.
13. **Khan, A. a, Dragt, B. S., Porte, R. J. and Groothuis, G. M. M.** (2010). Regulation of VDR expression in rat and human intestine and liver--consequences for CYP3A expression. *Toxicol. In Vitro* **24**, 822–9.
14. **Kidd, M., Modlin, I. M., Shapiro, M. D., Camp, R. L., Mane, S. M., Usinger, W. and Murren, J. R.** (2007). CTGF, intestinal stellate cells and carcinoid fibrogenesis. *World J. Gastroenterol.* **13**, 5208–16.

15. **Kitamura, H., Yamamoto, S., Nakase, H., Matsuura, M., Honzawa, Y., Matsumura, K., Takeda, Y., Uza, N., Nagata, K. and Chiba, T.** (2011). Role of heat shock protein 47 in intestinal fibrosis of experimental colitis. *Biochem. Biophys. Res. Commun.* **404**, 599–604.

16. **Kropski, J. a., Lawson, W. E. and Blackwell, T. S.** (2012). Right place, right time: the evolving role of herpesvirus infection as a "second hit" in idiopathic pulmonary fibrosis. *AJP Lung Cell. Mol. Physiol.* **302**, L441–L444.

17. **Kuang, P.-P., Zhang, X.-H., Rich, C. B., Foster, J. a, Subramanian, M. and Goldstein, R. H.** (2007). Activation of elastin transcription by transforming growth factor-beta in human lung fibroblasts. *Am. J. Physiol. Lung Cell. Mol. Physiol.* **292**, L944–L952.

18. **Kutz, S. M., Hordines, J., McKeown-Longo, P. J. and Higgins, P. J.** (2001). TGF-beta1-induced PAI-1 gene expression requires MEK activity and cell-to-substrate adhesion. *J. Cell Sci.* **114**, 3905–3914.

19. **Latella, G., Sferra, R., Speca, S., Vetuschi, A. and Gaudio, E.** (2013). Can we prevent, reduce or reverse intestinal fibrosis in IBD? *Eur. Rev. Med. Pharmacol. Sci.* **17**, 1283–304.

20. **Li, D. and Friedman, S. L.** (1999). Liver fibrogenesis and the role of hepatic stellate cells: new insights and prospects for therapy. *J. Gastroenterol. Hepatol.* **14**, 618–33.

21. **Louis, E., Collard, A., Oger, A. F., Degroote, E., Aboul Nasr El Yafi, F. A. and Belaiche, J.** (2001). Behaviour of Crohn's disease according to the Vienna classification: changing pattern over the course of the disease. *Gut* **49**, 777–82.

22. **Lund, P. K. and Rigby, R. J.** (2008). What are the mechanisms of fibrosis in IBD? *Inflamm. Bowel Dis.* **14 Suppl 2**, S127–8.

23. **Niu, X., de Graaf, I. a M. and Groothuis, G. M. M.** (2013). Evaluation of the intestinal toxicity and transport of xenobiotics utilizing precision-cut slices. *Xenobiotica.* **43**, 73–83.

24. **Park, P. O., Haglund, U., Bulkley, G. B. and Fält, K.** (1990). The sequence of development of intestinal tissue injury after strangulation ischemia and reperfusion. *Surgery* **107**, 574–80.

25. **Possidente, M., Dragoni, S., Franco, G., Gori, M., Bertelli, E., Teodori, E., Frosini, M. and Valoti, M.** (2011). Rat intestinal precision-cut slices as an *in vitro* model to study xenobiotic interaction with transporters. *Eur. J. Pharm. Biopharm.* **79**, 343–8.

26. **Rhyu, D. Y., Yang, Y., Ha, H., Lee, G. T., Song, J. S., Uh, S. and Lee, H. B.** (2005). Role of reactive oxygen species in TGF-beta1-induced mitogen-activated protein kinase activation and epithelial-mesenchymal transition in renal tubular epithelial cells. *J. Am. Soc. Nephrol.* **16**, 667–675.

27. **Rieder, F. and Fiocchi, C.** (2008). Intestinal fibrosis in inflammatory bowel disease - Current knowledge and future perspectives. *J. Crohns. Colitis* **2**, 279–90.

28. **Rieder, F. and Fiocchi, C.** (2009). Intestinal fibrosis in IBD--a dynamic, multifactorial process. *Nat. Rev. Gastroenterol. Hepatol.* **6**, 228–35.

29. **Rieder, F., Brenmoehl, J., Leeb, S., Schölmerich, J. and Rogler, G.** (2007). Wound healing and fibrosis in intestinal disease. *Gut* **56**, 130–9.

30. **Rieder, F., Kessler, S., Sans, M. and Fiocchi, C.** (2012). Animal models of intestinal fibrosis: new tools for the understanding of pathogenesis and therapy of human disease. *Am. J. Physiol. Gastrointest. Liver Physiol.* **303**, G786–801.

31. **Roskott, A. M., Nieuwenhuijs, V. B., Leuvenink, H. G. D., Dijkstra, G., Ottens, P., de Jager, M. H., Gonalves Dias Pereira, P., Fidler, V., Groothuis, G. M. M., Ploeg, R. J., et al.** (2010). Reduced ischemia-reoxygenation injury in rat intestine after luminal preservation with a tailored solution. *Transplantation* **90**, 622–9.

32. **Silverstein, M. D., Loftus, E. V, Sandborn, W. J., Tremaine, W. J., Feagan, B. G., Nietert, P. J., Harmsen, W. S. and Zinsmeister, A. R.** (1999). Clinical course and costs of care for Crohn's disease: Markov model analysis of a population-based cohort. *Gastroenterology* **117**, 49–57.

33. **Smith, P. D., Smythies, L. E., Shen, R., Greenwell-Wild, T., Gliozzi, M. and Wahl, S. M.** (2011). Intestinal macrophages and response to microbial encroachment. *Mucosal Immunol.* **4**, 31–42.

34. **Taguchi, T. and Razzaque, M. S.** (2007). The collagen-specific molecular chaperone HSP47: is there a role in fibrosis? *Trends Mol. Med.* **13**, 45–53.

35. **Taguchi, T., Nazneen, A., Al-Shihri, A. a, Turkistani, K. a and Razzaque, M. S.** (2011). Heat shock protein 47: a novel biomarker of phenotypically altered collagen-producing cells. *Acta Histochem. Cytochem.* **44**, 35–41.

36. **To, W. S. and Midwood, K. S.** (2011). Plasma and cellular fibronectin: distinct and independent functions during tissue repair. *Fibrogenesis Tissue Repair* **4**, 21.

37. **van de Bovenkamp, M., Groothuis, G. M. M., Meijer, D. K. F., Slooff, M. J. H. and Olinga, P.** (2006). Human liver slices as an *in vitro* model to study toxicity-induced hepatic stellate cell activation in a multicellular milieu. *Chem. Biol. Interact.* **162**, 62–9.

38. **van de Kerkhof, E. G., Ungell, A.-L. B., Sjöberg, A. K., de Jager, M. H., Hilgendorf, C., de Graaf, I. A. M. and Groothuis, G. M. M.** (2006). Innovative methods to study human intestinal drug metabolism *in vitro*: precision-cut slices compared with ussing chamber preparations. *Drug Metab. Dispos.* **34**, 1893–902.

39. **van de Kerkhof, E. G., de Graaf, I. A. M., de Jager, M. H. and Groothuis, G. M. M.** (2007). Induction of phase I and II drug metabolism in rat small intestine and colon *in vitro*. *Drug Metab. Dispos.* **35**, 898–907.

40. **van de Kerkhof, E. G., de Graaf, I. A. M., Ungell, A.-L. B. and Groothuis, G. M. M.** (2008a). Induction of metabolism and transport in human intestine: validation of precision-cut slices as a tool to study induction of drug metabolism in human intestine *in vitro*. *Drug Metab. Dispos.* **36**, 604–13.

41. **van de Kerkhof, E. G., de Graaf, I. A. M., Ungell, A.-L. B. and Groothuis, G. M. M.** (2008b). Induction of metabolism and transport in human intestine: validation of precision-cut slices as a tool to study induction of drug metabolism in human intestine *in vitro*. *Drug Metab. Dispos.* **36**, 604–13.

42. **Vickers, A. E. M. and Fisher, R. L.** (2005). Precision-cut organ slices to investigate target organ injury. *Expert Opin. Drug Metab. Toxicol.* **1**, 687–99.

43. **Westra, I. M., Oosterhuis, D., Groothuis, G. M. and Olinga, P.** (2011). Induction of fibrotic markers in an *in vitro* model of liver fibrosis. *Hepatology* **54**, 754A–755A.

44. **Westra, I. M., Pham, B. T., Groothuis, G. M. M. and Olinga, P.** (2013). Evaluation of fibrosis in precision-cut tissue slices. *Xenobiotica* **43**, 98–112.

45. **Westra, I. M., Oosterhuis, D., Groothuis, G. M. M. and Olinga, P.** (2014a). Precision-cut liver slices as a model for the early onset of liver fibrosis to test antifibrotic drugs. *Toxicol. Appl. Pharmacol.* **274**, 328–338.

46. **Westra, I. M., Oosterhuis, D., Groothuis, G. M. M. and Olinga, P.** (2014b). The Effect of Antifibrotic Drugs in Rat Precision-Cut Fibrotic Liver Slices. *PLoS One* **9**, e95462.

47. **Yan, F., Wang, Y., Wu, X., Peshavariya, H. M., Dusting, G. J., Zhang, M. and Jiang, F.** (2014). Nox4 and redox signaling mediate TGF-β-induced endothelial cell apoptosis and phenotypic switch. *Cell Death Dis.* **5**, e1010.